

Pinned and bound collective-mode state in charge-density-wave condensates

L. Degiorgi and G. Grüner

Department of Physics and Solid State Science Center, University of California at Los Angeles, Los Angeles, California 90024

(Received 1 April 1991)

We have studied the complete electrodynamic response of the model charge-density-wave compounds $K_{0.3}Mo_{1-x}W_xO_3$ ($x=0$ and 0.015), $(TaSe_4)_2I$ and TaS_3 by combining various optical experiments conducted in a broad spectral range. Our analysis leads to two distinct resonances in the dc far-infrared (FIR) spectral range. We argue that the first resonance, at the so-called pinning frequency, is due to the oscillatory response of the collective mode and suggest that the FIR optical mode is due to a bound collective-mode resonance, analogous to bound phonon states in semiconductors. We discuss a simple phenomenological approach, based on a Clausius-Mossotti-type model, and evaluate the parameters that characterize the FIR mode.

I. INTRODUCTION

The electrostatics of the charge-density-wave (CDW) ground state has been by now thoroughly explored, and several important features of this broken-symmetry ground state have been identified.¹ The complete excitation spectrum of the CDW condensates is characterized by both the single-particle gap (Δ) and the collective-mode contribution to the frequency-dependent conductivity. The former excitation is clearly evident in the infrared spectral range, while the collective response of the pinned CDW mode occurs usually at micro- or millimeter-wave frequencies. The collective-mode excitation is shifted from zero to finite frequency ω_0 because of the interaction with the lattice imperfections, and its dynamics is characterized by a large effective mass m^* . Consequently, the spectral weight of the collective mode is expected to be very small, of the order of m_b/m^* , where m_b is the band mass.¹ Furthermore, the study of the ac response in the MHz range is suggestive of different relaxation effects of the pinned mode. The so-called internal deformations are important for low-frequency processes, but they do not play a role for the high-frequency response.^{2,3} The CDW ground state of the model compound $K_{0.3}MoO_3$ is also characterized by several intense phonon peaks, which are clearly associated with the dynamical response of the collective mode and are ascribed to the so-called phase phonons.³

Recently, by combining various experimental techniques covering a broad spectral energy range, it was possible to identify a new resonance in the far infrared (FIR) above ω_0 but below the typical phonon frequencies. This FIR mode was clearly recognized in the CDW compounds $(TaSe_4)_2I$ and $K_{0.3}MoO_3$,^{4,5} while its appearance in TaS_3 was somewhat controversial.⁶ However, by combining our results at millimeter, microwave, and radio frequencies with optical results on TaS_3 ,⁶ the mode, although weak, also appears to exist in this material.⁷

Current models do not explain this resonance, which seems to be a universal or generic feature of all CDW condensates. We suggest that it occurs due to the bound CDW states, analogous to bound phonon states in semiconductors.

The aim of the present paper is to systematically review both the experimental results concerning the excitation spectrum of those CDW systems from the millimeter and microwave up to the far-infrared spectral range, as well as the theoretical understanding of the FIR mode. In Sec. II we will describe the various experimental techniques and the results of our investigations on $K_{0.3}MoO_3$ and its W alloys, on $(TaSe_4)_2I$, and on TaS_3 . In Sec. III we first compare our results with previous theoretical approaches, while in the second part we discuss our phenomenological model, based on an effective-medium theory of the dielectric function. Finally, our conclusions are summarized in Sec. IV. Some of our results have been reported earlier.^{3,4,7}

II. EXPERIMENT AND RESULTS

We have studied the complete electrodynamic response of $K_{0.3}Mo_{1-x}W_xO_3$ ($x=0$ and 0.015), $(TaSe_4)_2I$, and TaS_3 by combining various optical experiments conducted over a broad spectral range. The experiments were conducted at temperatures well below the transition temperature T_p [180, 265, and 220 K for $K_{0.3}MoO_3$, $(TaSe_4)_2I$, and TaS_3 , respectively] where the charge-density-wave state develops. In all experiments the electric-field direction was along the chain direction where the CDW modulation occurs. The components of the optical conductivity [$\sigma(\omega)=\sigma_1-i\sigma_2$] were measured directly up to frequencies 5 cm^{-1} by using micro- and millimeter-wave configurations.⁸ The components σ_1 and σ_2 were used to evaluate the reflectivity $R(\omega)$ using the expression

$$R(\omega) = \frac{1 + (4\pi/\omega)(\sigma_1^2 + \sigma_2^2)^{1/2} - 2\{(2\pi/\omega)[(\sigma_1^2 + \sigma_2^2)^{1/2} + \sigma_2]\}^{1/2}}{1 + (4\pi/\omega)(\sigma_1^2 + \sigma_2^2)^{1/2} + 2\{(2\pi/\omega)[(\sigma_1^2 + \sigma_2^2)^{1/2} + \sigma_2]\}^{1/2}}, \quad (1)$$

where ϵ_∞ (i.e., the $\omega \rightarrow \infty$ contribution to the dielectric constant) has been neglected, since ϵ_∞ is significantly small (i.e., $\approx 10^2$) in comparison to the actual value of the dielectric function $\epsilon_1(\omega)$ (i.e., $\approx 10^4$) in the GHz frequency range.³

$R(\omega)$ was then combined with optical reflectivity measurements over a broad spectral energy range between the FIR and ultraviolet (UV).^{3,5} In order to cover the whole energy range, different spectrometers were used with overlapping energy intervals. In the FIR we made use of a Michelson Fourier spectrometer with bolometric detectors. For the $\text{K}_{0.3}\text{Mo}_{1-x}\text{W}_x\text{O}_3$ compounds we conducted detailed optical measurements,³ while for TaS_3 and $(\text{TaSe}_4)_2\text{I}$ we combined our millimeter and microwave data^{8,9} with the optical results of Refs. 6 and 10, respectively. An exhaustive exposition of the various optical techniques employed is given in the mentioned literature, where the reader may find a detailed description of the crystal-growth procedures as well.

In Fig. 1 we display the complete $R(\omega)$ spectrum for the three investigated CDW condensates. As we will discuss in more detail below, the optical reflectivity measured down to the far infrared [i.e., $\approx 15 \text{ cm}^{-1}$ or even lower to $\approx 10 \text{ cm}^{-1}$ as in the case of TaS_3 (Ref. 6)] was matched to the reflectance data gained from the direct measurement of σ_1 and σ_2 in the micro- and millimeter-wave spectral energy range.³

In view of the main purpose of the present work, we concentrate our attention on the spectral energy range between dc and 100 cm^{-1} . An attentive inspection of Fig. 1 shows that in all cases the reflectivity R is different from 100% as $\omega \rightarrow 0$, rises to a maximum in the millimeter-wave range, followed by a local minimum at higher frequencies. This general behavior is well magnified in Fig. 2(a), where, as an example, the $R(\omega)$ between dc and 100 cm^{-1} for $\text{K}_{0.3}\text{MoO}_3$ is reported. The solid circles represent the $R(\omega)$ values evaluated in the micro- and millimeter-wave spectral range using Eq. (1), while the dashed line at frequencies below $\approx 14 \text{ cm}^{-1}$ has been obtained by fitting the micro- and millimeter-wave results with several harmonic oscillators. The behavior of the reflectivity described above is characteristic of two resonances. In order to demonstrate this we have calculated $R(\omega)$ by assuming that σ is composed of two oscillators with different parameters,⁴ i.e.,

$$\sigma(\omega) = \frac{\omega_{p0}^2}{4\pi} \frac{i\omega}{\omega^2 - \omega_0^2 + i\omega/\tau_0} + \frac{\omega_{p1}^2}{4\pi} \frac{i\omega}{\omega^2 - \omega_1^2 + i\omega/\tau_1} - i\frac{\omega}{4\pi} \epsilon_\infty, \quad (2)$$

where $\omega_\pi^2/8$ represents the oscillator strength associated

with each resonance and ϵ_∞ is the contribution from optical structures at higher frequencies.

Figure 2(b) shows the calculated $R(\omega)$ for $\text{K}_{0.3}\text{MoO}_3$, where the parameters ω_i , ω_{pi} , $1/\tau_i$ for the two resonances are 3.33 , 834 , and 0.67 cm^{-1} and 26.7 , 1334 , and 2.67 cm^{-1} , respectively, and $\epsilon_\infty = 600$. All the experimental findings are well reproduced, and as we stressed previously,⁴ the lower-frequency range of all CDW condensates can be recovered only if both resonances simultaneously make a contribution to the reflectivity. In Fig. 2(b) we

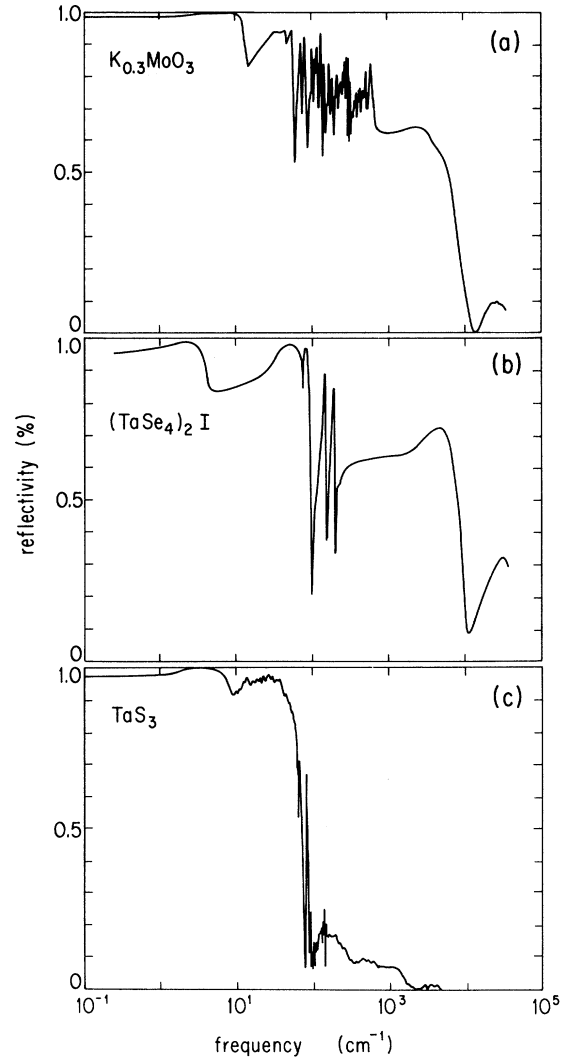


FIG. 1. Complete reflectivity spectrum $R(\omega)$ at 6 K of (a) $\text{K}_{0.3}\text{MoO}_3$, (b) $(\text{TaSe}_4)_2\text{I}$, and (c) TaS_3 , for polarization parallel to the conducting chains.

have also described the two phonon modes above the FIR resonance (ω_1) in terms of harmonic oscillators (with 71.7 and 83.4 cm^{-1} for the frequencies, 333.6 and 500 cm^{-1} for the mode strengths, and 1.33 and 1.67 cm^{-1} for the dampings, respectively).

The reflectivity, displayed in Fig. 1, was subsequently used for the Kramers-Kronig (KK) analysis, from which we can evaluate the complete ac conductivity. In Fig. 3 we show $\sigma_1(\omega)$ for the three investigated compounds in the spectral energy range from dc to the FIR. The two resonances clearly appear as independent oscillators. In Fig. 3 we show also the experimental millimeter and microwave points for $\text{K}_{0.3}\text{MoO}_3$ and furthermore the optical conductivity for the W-doped ($x=0.015$) compound. Finally, it is interesting to remark that, while the first resonance moves to higher frequency upon doping, the position of the FIR one is only slightly modified.

III. DISCUSSION

Our experimental results clearly identify two resonances in the excitation spectrum from dc to the FIR in

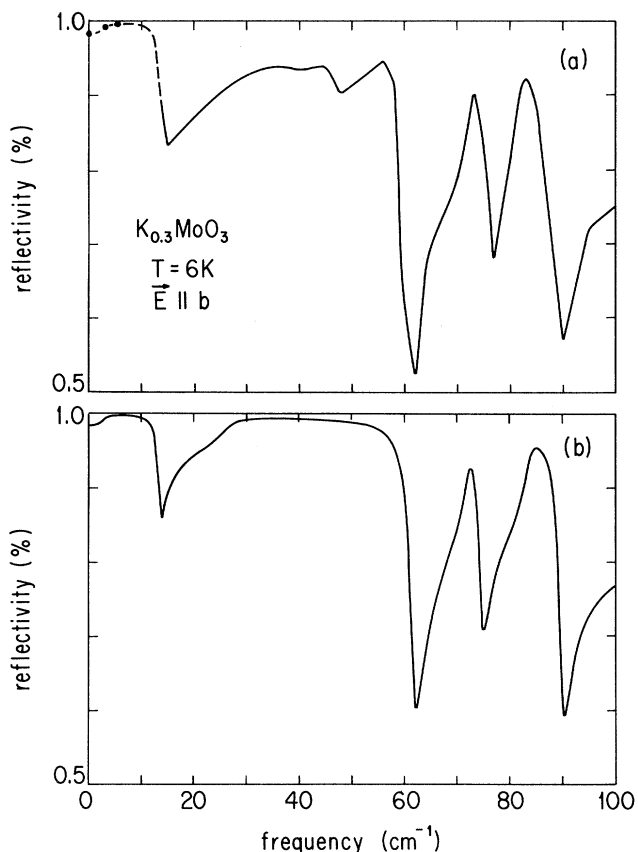


FIG. 2. (a) Reflectivity R vs frequency in the radio-to-infrared spectral range for $\text{K}_{0.3}\text{MoO}_3$. Circles are the micro- and millimeter-wave data using Eq. (1). The dashed line represents the calculated reflectivity within the harmonic-oscillator approach (see text). (b) Calculated reflectivity for four harmonic oscillators. The parameters used to calculate $R(\omega)$ are given in the text.

all three CDW condensates. The first resonance occurs at $\omega_0 = 1.5 \text{ cm}^{-1}$ for TaS_3 and $(\text{TaSe}_4)_2\text{I}$ and at 3.33 cm^{-1} for $\text{K}_{0.3}\text{MoO}_3$, and it is ascribed to the oscillatory response of the collective mode. There is evidence to support this assignment, and an extensive discussion may be found in the literature.¹ Here we only wish to stress two points. First, our experiments on doped specimens clearly demonstrate the shift of the resonance frequency with increased doping, as expected for impurity pinning [Fig. 3(a)].^{1,4,5,9} Second, the effective mass m^* associated with this resonance can be evaluated from the measured oscillator strength of the resonance ($\omega_{p0}^2/8$). One obtains an effective mass m^* significantly larger than the band mass (i.e. in the order of magnitude between 10^2 and 10^4), which reflects the response of the coupled electron-

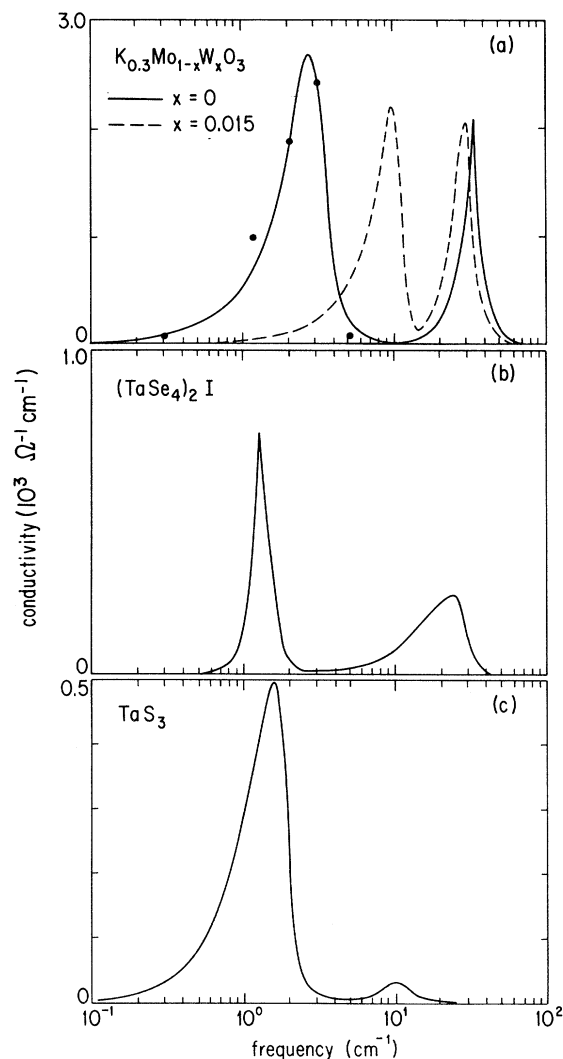


FIG. 3. Optical conductivity from the microwave-to-FIR spectral range, as evaluated from Kramers-Kronig analysis, for (a) $\text{K}_{0.3}\text{MoO}_3$ and one of its alloys, (b) $(\text{TaSe}_4)_2\text{I}$, and (c) TaS_3 . In (a) we show also the millimeter and microwave experimental points (circles) for the pure blue bronze.

phonon system to central perturbations. The obtained values for m^* are also in fair agreement with the mean-field result.^{4,11} A more detailed analysis of the value of m^* will be discussed later.

The second resonance which occurs at $\omega_1 = 10 \text{ cm}^{-1}$ in TaS₃, at 40 cm^{-1} in K_{0.3}MoO₃, and at 38 cm^{-1} in (TaSe₄)₂I has not been yet identified, although several modes above ω_0 and below Δ/\hbar may be associated with the various excitations of the charge-density-wave condensate, and a large amount of both theoretical and experimental work was performed in an attempt to understand this resonance. One might be tempted to ascribe this resonance to the FIR component of the amplitude mode. The amplitude mode is Raman, but not infrared active in specimens without lattice imperfections.¹¹ However, impurities, which pin the collective mode, could, by breaking the translational symmetry, lead to a finite polarization accompanying the amplitude fluctuations. Such a mechanism would then lead to an optical resonance at the amplitude-mode frequency ω_A . This frequency has been measured in K_{0.3}MoO₃ at $\omega_A = 57 \text{ cm}^{-1}$ (Ref. 12) and in (TaSe₄)₂I at $\omega_A = 90 \text{ cm}^{-1}$,¹³ while for TaS₃ we estimate $\omega_A = 77 \text{ cm}^{-1}$ within a mean-field approach where $2\Delta = 2420 \text{ cm}^{-1}$ (0.3 eV) and m^*/m of the order of 10^3 were assumed (see below).^{1,6} As far as the single-particle gap of TaS₃ is concerned, there is not any unanimity about its value. Following the estimation of Tsang, Hermann, and Shafer [i.e., $2\Delta = 536 \text{ cm}^{-1}$ (0.067 eV)], we would obtain a value of $\omega_A = 20 \text{ cm}^{-1}$, which might be considered as lower limit for the amplitude-mode frequency.¹⁴ In all cases ω_A is significantly higher than the frequency of the FIR resonances shown in Fig. 3. Therefore, we consider this mechanism unlikely. Moreover, the frequency of the amplitude mode is a lower-bound frequency for any other possible phonon mode. For instance, a look at the phonon-dispersion relation of K_{0.3}MoO₃ (Ref. 15) is enough to convince oneself that it is very unrealistic to expect ordinary FIR active phonon excitations below ω_A . Furthermore, bare Raman-active phonons, which may be FIR activated by the electron-phonon coupling to the CDW condensate as suggested by the phase-phonon model,¹⁶ are also not expected in this range.

It has been also suggested,¹⁰ that the resonance in (TaSe₄)₂I is due to an optical phason, which arises due to a periodicity $\lambda = \pi/k_F$, leading to a $q = 2k_F$ optically active mode. The relevant frequency is $\omega_{\text{op}} = (1/m_b m^*)^{1/2} (4\pi\hbar/\lambda^2)$, where λ is the period of the CDW, $\lambda = 14 \text{ \AA}$ for K_{0.3}MoO₃ and TaS₃, and 16 \AA for (TaSe₄)₂I.¹ As the effective masses are widely different, ω_{op} is expected to differ by approximately a factor of 6 between K_{0.3}MoO₃, and TaS₃ and (TaSe₄)₂I,¹ in clear disagreement with the experimental observations.

Another possibility arises if one takes into account the Coulomb effects. The latter ones are important at low temperature, where screening by normal electrons is absent, and consequently the phason dispersion relation develops a gap at $q=0$. In other words, inclusion of Coulomb interactions leads to a long-wavelength phase-mode spectrum consisting of an acoustical and optical

branch.¹⁷ However, the optical-mode frequency ($\tilde{\omega}$) is expected to be even higher than the amplitude-mode one [i.e., $\tilde{\omega} \approx (\frac{3}{2})^{1/2} \omega_A$]. Thus we consider this possibility extremely unlikely.

Finally, for charge-density waves near to commensurability, a midgap band inside the main Peierls gap appears because of the so-called soliton lattice.¹⁸ Such effects could be important in K_{0.3}MoO₃, which is a nearly commensurate CDW system. However, the resonance frequency associated with these midgap states is approximately one order of magnitude larger than the observed frequencies. Thus we argue that none of these interpretations can be clearly identified as the FIR resonance we have observed.

In the following subsections, we will discuss our phenomenological approach,⁷ which takes into account both the pinned CDW and FIR resonance. In Sec. III A we will present the model, while its systematic application to the investigated CDW compounds will be discussed in Sec. III B.

A. Phenomenological model

We propose a Clausius-Mossotti-type description of the dielectric function characterizing the electrodynamic response of a CDW condensate.^{19,20} We consider a bulk medium, with dielectric function $\epsilon_m(\omega)$, which contains spherical regions of radius r_s , due to impurities or defects, with a different dielectric function $\epsilon_s(\omega)$. The following derivation of the effective-medium dielectric function is perfectly general and does not depend on the exact form of ϵ_s . First, we consider the relative situation where the spheres of dielectric function $\epsilon = \epsilon_s/\epsilon_m$ reside in a medium with dielectric function 1. The standard approach for a random distribution of such (nonoverlapping) polarizable spheres leads to the dielectric function

$$\epsilon_{\text{gas}} = 1 + \frac{4\pi N_s \alpha}{1 - (4\pi/3) N_s \alpha}, \quad (3)$$

where α is the polarizability of each sphere and N_s their density.²¹ One can also evaluate the polarization of the spheres from their dipole moment induced by the local field. It is then straightforward to recover the polarizability α :

$$\alpha = \frac{r_s^3 (\epsilon - 1)}{(\epsilon + 2)}. \quad (4)$$

Finally, substitution of Eq. (4) in Eq. (3) gives the effective-medium dielectric function of the system as

$$\epsilon_{\text{eff}} = \epsilon_m + \frac{3\epsilon_m (\epsilon_s - \epsilon_m) f}{\epsilon_s + 2\epsilon_m - (\epsilon_s - \epsilon_m) f}, \quad (5)$$

where we have removed the relative dielectric function ϵ by multiplying with ϵ_m and we have made use of the relation $f = N_s (4\pi/3) r_s^3$ for the dimensionless filling factor.

Examination of Eq. (5) shows that, if the spheres are absent ($f=0$), the dielectric function reverts to ϵ_m as expected, while, for finite f , ϵ_{eff} has a transverse mode at the pole of $\epsilon_m(\omega)$ (as it has for $f=0$) and also near the

frequency where $\epsilon_s = -2\epsilon_m$. This latter mode defines a localized resonance centered on the spheres.

In the frequency range of interest for the present discussion, the frequency-dependent dielectric function of the bulk medium [$\epsilon_m(\omega)$] is dominated by the resonance of the pinned CDW mode. A harmonic oscillator has been used extensively to describe the dielectric function of the CDW collective mode:⁴

$$\epsilon_m(\omega) = \epsilon_\infty + \frac{\omega_{p0}^2}{\omega_0^2 - \omega^2 - i\omega\gamma}, \quad (6)$$

where, as usual, ω_0 is the resonance frequency, γ the damping, and ω_{p0} the plasma frequency. The frequency-independent constant ϵ_∞ takes into account the high-frequency contribution to $\epsilon_m(\omega)$. Furthermore, we assume that around each impurity the dielectric function is given by

$$\epsilon_s(\omega) = \epsilon_m(\omega) + \epsilon_0. \quad (7)$$

The origin of the frequency-independent term ϵ_0 will be discussed later.

As an example, we show in Fig. 4(a) the real part of $\epsilon_{\text{eff}}(\omega)$ after Eqs. (5)–(7), while Fig. 4(b) displays the so-called energy-loss spectrum [$\text{Im}(-1/\epsilon_{\text{eff}})$] with parameters for $\text{K}_{0.3}\text{MoO}_3$ (see Table I). The extra polarizability around the impurities (i.e., within the spheres) locally perturbs the dielectric function, and $\epsilon_{\text{eff}}(\omega)$ has then two zero crossings: one at ω_{LO} [i.e., where $\epsilon_m(\omega) = 0$ and $d\epsilon_m/d\omega > 0$] and one at $\omega < \omega_{\text{LO}}$ (Fig. 4). This situation leads to a new absorption in the excitation spectrum and closely parallels what happens in the case of lightly doped semiconductors; ω_{LO} would correspond to the longitudinal-optical-phonon mode, while the mode appearing below ω_{LO} would be ascribed to the additional zero crossing which follows from Eq. (5). This latter resonance is generally called the bound-phonon mode, and consequently we call the FIR resonance (ω_1) which appears above the pinned CDW mode (ω_0) the bound collective-mode resonance.

B. Application to CDW condensates

Using the former phenomenological approach, we have calculated the optical conductivity $\sigma_1(\omega) = (\omega/4\pi)\text{Im}[\epsilon_{\text{eff}}(\omega)]$ for the three investigated CDW compounds. Figure 5 systematically shows the result of our calculations using the parameters which are summarized in Table I. With this set of parameters we obtain fair

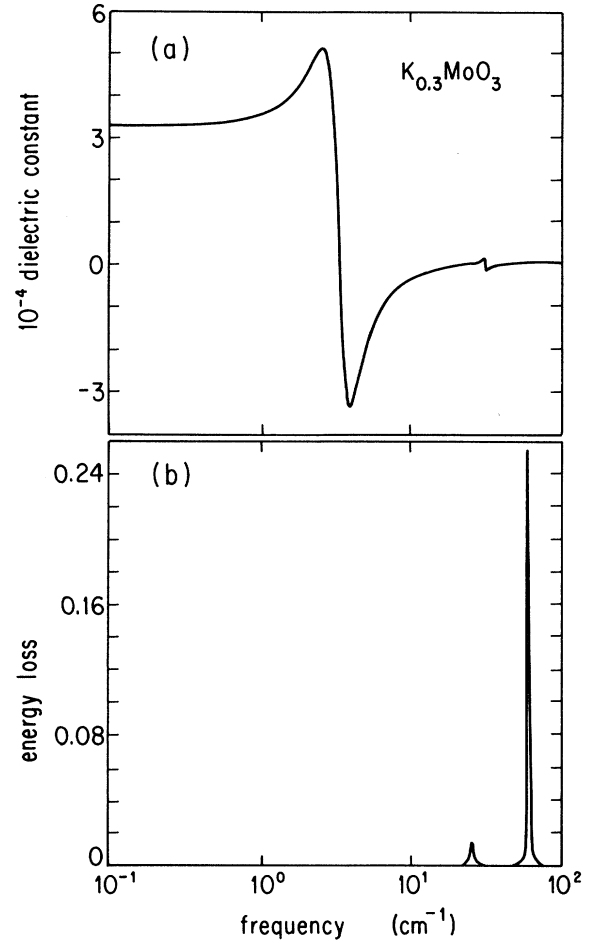


FIG. 4. (a) Effective dielectric function calculated for $\text{K}_{0.3}\text{MoO}_3$ using Eq. (5) and (b) the corresponding energy-loss spectrum.

agreement with the experimental results of Fig. 3. For $\text{K}_{0.3}\text{MoO}_3$ we also remark that the parameters defining the pinned CDW mode are very close to those used previously for the phenomenological description of the $R(\omega)$ spectrum in terms of harmonic oscillators. Next, we discuss the values in Table I, comparing them with various experimental data.

First, the plasma frequency ω_{p0} leads to a dynamical mass enhancement $m^*/m = 720$, 3000, and 500 for $\text{K}_{0.3}\text{MoO}_3$, $(\text{TaSe}_4)_2\text{I}$, and TaS_3 , respectively, in fair

TABLE I. Parameters used for the model calculation: the frequency of the pinned mode (ω_0), the damping constant (γ), the plasma frequency (ω_{p0}), the high-frequency contribution (ϵ_∞), the impurity contribution (ϵ_0) to the dielectric function, and the filling factor (f), all in cm^{-1} , and the restoring force ($k = m^* \omega_0^2$) of the pinned mode, in $(\text{cm}^{-1})^2$.

	ω_0	γ	ω_{p0}	ϵ_∞	ϵ_0	f	$m^* \omega_0^2$
$\text{K}_{0.3}\text{MoO}_3$	3.33	1.34	600	100	1000	0.2	7 984
$\text{K}_{0.3}\text{Mo}_{0.985}\text{W}_{0.015}\text{O}_3$	10.0	1.34	600	300	1000	0.8	72 000
$(\text{TaSe}_4)_2\text{I}$	2.0	2.0	300	50	190	0.2	12 000
TaS_3	2.0	0.66	189	100	1000	0.05	2 000

agreement with the values obtained earlier using $\sigma_1(\omega)$ data in the micro- and millimeter-wave spectral range alone.¹ The former values are calculated from the ratio $(\omega_p/\omega_{p0})^2 \approx m^*/m$, where ω_p is the plasma frequency of the normal or uncondensed electrons, which actually describes the total spectral weight. Furthermore, we can compare our m^*/m with the mean-field estimated values.^{1,11} In fact, at least for $\text{K}_{0.3}\text{MoO}_3$ and $(\text{TaSe}_4)_2\text{I}$ it is possible to recover m^*/m from the expression

$$\frac{m^*}{m} = 1 + (2\Delta/\omega_A)^2, \quad (8)$$

where 2Δ is the single-particle gap and ω_A the amplitude-mode frequency. With $2\Delta = 1613 \text{ cm}^{-1}$ (0.2 eV) and 4000 cm^{-1} (0.5 eV) and $\omega_A = 57$ and 90 cm^{-1} , we obtain $m^*/m \approx 800$ and 2000 for $\text{K}_{0.3}\text{MoO}_3$ and $(\text{TaSe}_4)_2\text{I}$, respectively. Since the estimation of ω_A for TaS_3 was precisely obtained from Eq. (8), the same comparison here would be redundant.

Our earlier experiments with alloys of $\text{K}_{0.3}\text{MoO}_3$, $(\text{TaSe}_4)_2\text{I}$, and TaS_3 suggest an overall residual impurity concentration N_s of approximately 10^{18} cm^{-3} .^{5,9,22} The f values given in Table I imply a characteristic radius r_s of about 40 \AA , a value fairly comparable with typical r_s values in the semiconductors (i.e., around 30 \AA).¹⁹ Moreover, within a recent strong-pinning theory of CDW dynamics, our r_s is in a good agreement with the length scale $[\xi_{\parallel}(A_0/2\xi_{\perp}^2)]^{1/2}$; ξ_{\parallel} represents the CDW-amplitude coherence length along the chain direction and ξ_{\perp} in the transverse direction, and A_0 is the cross-sectional area] corresponding to a volume surrounding the individual impurity sites, where the adjustment between the average CDW phase and the pinned value takes place.²³ The factor of 4 between the filling factor of TaS_3 and those of the other materials is explained by slightly different actual values of N_s and r_s , which indeed should easily accommodate that difference. We note that the above considerations are also strongly supported by our experiments and our model approach on $\text{K}_{0.3}\text{Mo}_{1-x}\text{W}_x\text{O}_3$ with $x = 0.015$. The analysis of the optical data leaves the effective mass unchanged, but increases ω_0 and the filling factor f , as expected for increasing impurity concentration.

We have also calculated the normalized spectral intensity of the bound CDW mode, defined by the expression¹⁹

$$A = \frac{\int_{\text{bound CDW mode}} \text{Im}(-1/\epsilon_{\text{eff}})d\omega}{\int_{\text{pinned mode}} \text{Im}(-1/\epsilon_{\text{eff}})d\omega}, \quad (9)$$

where $\text{Im}(-1/\epsilon_{\text{eff}})$ is the so-called energy-loss spectrum [e.g., Fig. 4(b)]. Both A and f are expected to be proportional to the impurity concentration c to first order. We have shown earlier^{1,9} that the restoring force k acting on the collective mode is proportional to the impurity concentration, $k = ac$.²⁴ As $k = m^*\omega_0^2$, we expect c and consequently both A and f to be proportional to $m^*\omega_0^2$. In Fig. 6 we have plotted these two parameters versus k evaluated using the values for $m^*\omega_0^2$ given in Table I. The solid line indicates the linear relation between A , f and the parameter k (or, equivalently c), and consequently the figure clearly demonstrates that the FIR mode is associated with impurity states.

The dielectric constant ϵ_0 , characteristic of the volume $V = 4\pi r_s^3/3$ around the impurities, is significantly larger than $\epsilon_{\Delta} \sim 10^2$, which results from the single-particle transitions across the Peierls gap Δ . The large radius r_s and also the large dielectric constant ϵ_0 may arise as the consequence of several contributions. Assuming that a treatment appropriate for simple semiconductors applies, the polarizability α associated with the defects is given by

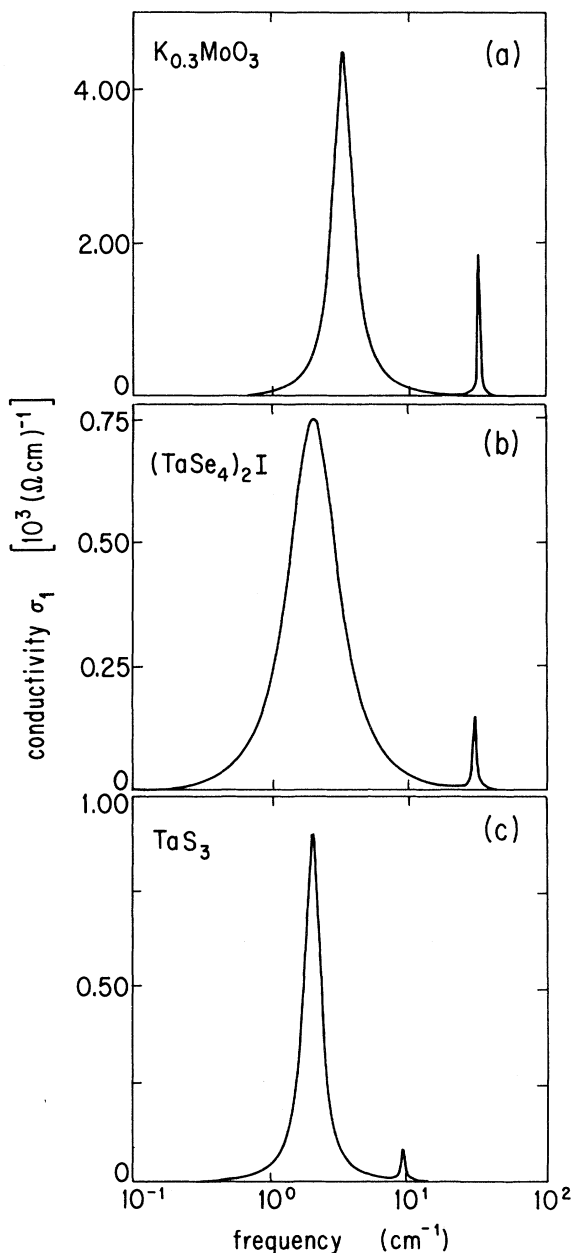


FIG. 5. Calculated optical conductivity $\sigma_1(\omega)$ after Eqs. (5)–(7) between 10^{-1} and 10^2 cm^{-1} for (a) $\text{K}_{0.3}\text{MoO}_3$, (b) $(\text{TaSe}_4)_2\text{I}$, and (c) TaS_3 . The parameters used for this phenomenological approach are summarized in Table I.

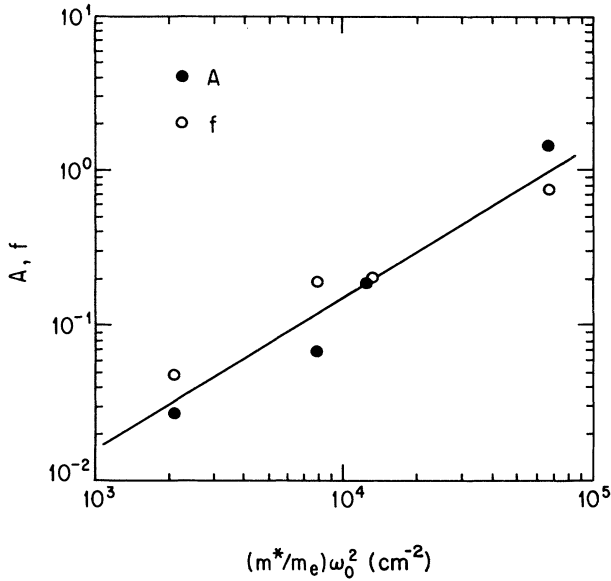


FIG. 6. Normalized spectral intensity A (●) and filling factor f (○) plotted vs the restoring force $k = m^* \omega_0^2$, using the values of Table I.

$\alpha = V(\epsilon_0 - 1)/4\pi$. The usual treatment of impurity states in semiconductors uses the vacuum polarizability of the H atom ($0.67 \times 10^{-24} \text{ cm}^3$) and the dielectric constant enhancement $\eta \sim \epsilon_\infty^4$ as input parameters.²⁵ We evaluated ϵ_∞ from our previous KK analysis,^{4,5} and obtain an estimation for ϵ_0 of about 3000 for $\text{K}_{0.3}\text{MoO}_3$ and TaS_3 and 200 for $(\text{TaSe}_4)_2\text{I}$. This is in agreement with our calculated values (Table I). Here it has to be remarked that our ϵ_∞ for TaS_3 is larger than the value proposed in Ref. 6. Nevertheless, we should point out the fairly important dependence of ϵ_∞ (which considers the high-frequency contributions from the FIR up to the Peierls gap) to the absolute value of the reflectivity. Since the optical measurements of TaS_3 and $(\text{TaSe}_4)_2\text{I}$ were performed on mosaic sample arrangements, we have to consider the non-negligible surface scattering. Such effects are of course important at higher frequencies, affecting then the evaluation of ϵ_1 and ϵ_2 . However, a fairly good simulation of the experimental $\sigma_1(\omega)$ for TaS_3 was also obtained with $\epsilon_\infty = 50$.

Furthermore, it is also envisaged that bound states, at frequencies below the gap frequency Δ/\hbar but well above the resonances discussed here, arise as the consequence of impurity-charge density-wave interactions.²⁶ Resonances associated with such defect bound states will contribute to the dielectric constant $\epsilon_s(\omega)$. Even though the oscillator strength of these resonances has not been calculated, it is expected that for low frequencies a significant contribution to ϵ_0 (exceeding ϵ_Δ) is recovered. In a similar way and as discussed before, a contribution to ϵ_s may also

arise from midgap bands, which will appear in CDW systems near commensurability.¹⁸

Finally, we remark that the experimental results show a broader FIR resonance than in the calculated spectrum (i.e., in analogy to the semiconductor problem, the bound mode should have localized character). We may ascribe the experimentally found broadening of the FIR mode to nonhomogeneities of the impurities distribution and of their pinning potential. Furthermore, we note that the present model approach does not contain any explicit temperature dependence. The thermal screening at higher temperature certainly broadens the low-frequency resonances and might be important in TaS_3 because of the weakness of the FIR resonance. One way to take into account such effects would be, e.g., to perform a Gaussian convolution. This, however, would not lead to important changes in the optical spectrum.

IV. CONCLUSION

We have examined the low-energy electrodynamic response of various charge-density-wave condensates and have found two resonances in the dc to FIR spectral range. We account for both resonances in terms of an effective-medium theory, which assumes that impurities lead to an excess dielectric constant within a region of radius r_s around the impurity sites. The large impurity-induced dielectric constant (exceeding ϵ_Δ originating from excitation across the single-particle gap) is due to impurity-induced resonances below the gap. Optical experiments in the spectral range somewhat below Δ , while highly suggestive of such resonances, are somehow controversial.^{27,28} Optical experiments which examine both the FIR region and spectral range near Δ would establish the relation between the bound resonances and FIR bound state we have explored. We also believe that the bound state discussed here is only one example of the interaction between a collective mode and impurities and that similar effects should occur in other incommensurate structures where the translational mode is optically active.

Finally, this work demonstrates once again how essential the combination of many experimental techniques, covering different frequency ranges, is for a reliable evaluation of the parameters characterizing the CDW ground state.

ACKNOWLEDGMENTS

We wish to thank A. Zettl and W. N. Creager for sending us copies of papers (Ref. 6) in advance of publication, as well as for useful discussions. The valuable help of Y. M. Kim is also acknowledged. The specimens used in this study were grown by B. Alavi. This research was supported by NSF Grant No. DMR 89-13236. One of us (L.D.) wishes to acknowledge the financial support of the Swiss National Science Foundation.

- ¹G. Grüner, *Rev. Mod. Phys.* **60**, 1129 (1988), and references cited therein.
- ²G. Mihály, T. W. Kim, and G. Grüner, *Phys. Rev. B* **39**, 13 009 (1989).
- ³L. Degiorgi, B. Alavi, G. Mihály, and G. Grüner, *Phys. Rev. B* **44**, 7808 (1991).
- ⁴S. Donovan, Y. Kim, B. Alavi, L. Degiorgi, and G. Grüner, *Solid State Commun.* **75**, 721 (1990).
- ⁵Y. Kim, L. Degiorgi, B. Alavi, and G. Grüner, *Synth. Met.* **41-43**, 3959 (1991).
- ⁶W. N. Creager, P. L. Richards, and A. Zettl, *Synth. Met.* **41-43**, 3867 (1991).
- ⁷L. Degiorgi and G. Grüner, *Europhys. Lett.* (to be published).
- ⁸S. Sridhar, D. Reagor, and G. Grüner, *Phys. Rev. B* **34**, 2223 (1986).
- ⁹T. W. Kim, S. Donovan, G. Grüner, and A. Phillipp, *Phys. Rev. B* **43**, 6315 (1991).
- ¹⁰M. S. Sherwin, A. Zettl, and P. L. Richards, *Phys. Rev. B* **36**, 708 (1987); H. R. Gesserich *et al.*, *Physica B* **143**, 198 (1986).
- ¹¹P. A. Lee, T. M. Rice, and P. W. Anderson, *Solid State Commun.* **14**, 703 (1974).
- ¹²G. Travaglini, I. Mörke, and P. Wachter, *Solid State Commun.* **45**, 289 (1983).
- ¹³S. Sugai, M. Sato, and S. Kurihara, *Phys. Rev. B* **32**, 6809 (1985).
- ¹⁴J. C. Tsang, C. Hermann, and M. W. Shafer, *Phys. Rev. Lett.* **40**, 1528 (1978).
- ¹⁵J. P. Pouget, in *Low Dimensional Electronic Properties of Molybdenum Bronze and Oxides*, edited by C. Schlenker (Kluwer Academic, Amsterdam, 1989), p. 87; *Phys. Rev. B* **43**, 3575 (1991).
- ¹⁶M. J. Rice, *Phys. Rev. Lett.* **37**, 36 (1976).
- ¹⁷K. W. Wong and S. Takada, *Phys. Rev. B* **36**, 5476 (1987).
- ¹⁸K. Machida and M. Nakano, *Phys. Rev. Lett.* **55**, 1927 (1985).
- ¹⁹A. S. Barker, Jr., *Phys. Rev. B* **7**, 2507 (1973).
- ²⁰L. Genzel and T. P. Martin, *Phys. Status Solidi* **51**, 91 (1972).
- ²¹J. D. Jackson, in *Classical Electrodynamics* (Wiley, New York, 1962), Chap. 4, p. 152.
- ²²D. Reagor and G. Grüner, *Phys. Rev. B* **39**, 7626 (1989).
- ²³W. G. Lyons and J. R. Tucker, *Phys. Rev. B* **38**, 4303 (1988).
- ²⁴ a is a numerical factor which depends on the impurity potential, transition temperature, and parameters of the metallic state above the transition. These parameters do not change dramatically from material to material, and we assumed a to be the same for all three compounds investigated.
- ²⁵J. J. O'Dwyer and H. H. Nickle, *Phys. Rev. B* **2**, 5063 (1970).
- ²⁶I. Túttó and A. Zawadowski, *Phys. Rev. B* **32**, 2449 (1985).
- ²⁷M. E. Itkis and F. Ya. Nad', *Pis'ma Zh. Eksp. Teor. Fiz.* **39**, 373 (1984) [*JETP Lett.* **39**, 448 (1984)].
- ²⁸G. Minton and J. W. Brill, *Synth. Met.* **29**, F481 (1989).